A Large Scale Network Model To Obtain Interwell Formation Characteristics

S.A. Gherabati[a,*], R.G. Hughes[a], C.D. White[a], H. Zhang[b]

[a] *Craft and Hawkins Department of Petroleum Engineering, Louisiana State University, Patrick F. Taylor, Baton Rouge, LA 70803*
[b] *Department of Mathematics, Louisiana State University, Baton Rouge, LA, 70803*

Abstract

Limited data availability and poor data quality make it difficult to characterize many reservoirs. For reservoirs that have undergone waterflooding, production and injection data are a reliable source of information from which injector-to-producer connections can be inferred. In this research, we use well locations and injection and production rate data to develop a reservoir-scale network model. The coarse network model approach is fast and efficient since it solves for a relatively small number of unknowns and is less underdetermined than correlation-based methods.

A Voronoi mesh divides the reservoir into a number of node volumes each of which contains a well. Bonds connect each of the nodes with conductance values that must be inferred from the rate data. An inverse problem is formulated where the mean-squared difference between the modeled and actual production data are minimized and the conductance values between each node are the unknowns. A derivative free optimization algorithm is utilized to minimize the objective function.

The application of this work is primarily for secondary and tertiary floods with limited geological data. The solution parameters are directly proportional to formation properties. This approach has been successfully tested for different synthetic permeability distribution cases and field injection scenarios. The main advantages of the proposed method are:

- It can model changes in flow pattern caused by adding new wells or shutting-in producers.

*Corresponding author, Tel: +1 225 2001735
Email address: sghera1@lsu.edu (S.A. Gherabati)

- It uses conventional history matching methods to solve a simplified inverse problem using only production and injection data. It uses a small number of nodes and converges to a better posed solution than statistical approaches. Convergence to a solution for higher frequency data only decreases the speed of the method slightly.

- The degree of injector to producer interaction is not fixed and can vary over time. Thus, the technique captures more of the physical relationships between well pairs and features that influence the dynamic behavior of the reservoir than previous correlation-based methods.

Keywords:
waterflooding, inter-well characterization, network model, conductance

---

1. Introduction

Studying the changes in well production rates as injection rates fluctuate gives insight about interwell formation characteristics. Local permeability values along with the potential gradient, controls the direction of fluid flow in a reservoir. History matching is the most common way of inferring the permeability distribution in a reservoir. History matching involves a cumbersome task of gathering and adjusting numerous data (permeability, porosity, saturation, seismic parameters ...) to match observed and simulated production rates and pressures. Because of the uncertainties associated with the data, detailed output models may not be realistic. Permeability distribution and barrier positions are two examples of reservoir properties and features that are always estimated with uncertainty unless there are enough core and well test data available. The simulation model behaves differently in terms of pressure and production response under different realizations of the model data. Therefore, in cases where knowledge of reservoir properties and conditions are limited, models with fewer, well understood parameters may answer questions more confidently than models with many uncertain parameters. For example, the resistance to flow between two points in the medium caused by 1000 block permeability values in a detailed model may be represented by a single parameter in the simple model. Such a parameter may help to reduce the uncertainties of complex models. Even for cases with enough certain data, a detailed answer may not always be necessary and a quick solution may sometimes suffice. In order to obtain such a solution, a

simplified model is needed which can be easily set up for different cases. The input to the model should be reliable with limited data manipulation and the output should have physical meaning.

Models that are based on the statistical correlation between injection and production rates have been shown to be practically useful to quantify reservoirs that have undergone waterflooding. Many methods have been proposed in this area. Refunjol and Lake (1997) used Spearman analysis and Panda and Chopra (1998) trained an artificial neural network to estimate injector-producer interaction. Albertoni and Lake (2003) implemented multivariate linear regression and diffusivity filters to describe connectivity between injection and production wells. In their model, production rates at a producing well were assumed to be a linear combination of the injection rates of every injector. Diffusivity filters were applied to injection rates to account for potential time lags between injection and the resulting production. In this work this will be referred to as a resistance model (RM). In order to resolve limitations of the Albertoni and Lake (2003) model, Yousef et al. (2006) proposed a more complex model, named the capacitance model (CM). They incorporated compressibility into this model in addition to transmissibility to quantify the degree of fluid storage between wells. This approach requires bottomhole pressure information in addition to rate data. To improve the CM, Kaviani et al. (2008) proposed a segmented CM for the cases where bottom hole pressure (BHP) data are unknown and a compensated capacitance model when a producer is added or shut-in. Sayarpour (2008) introduced capacitance-resistance models (CRM) in which he solved the fundamental differential equation of the capacitance model based on superposition in time. He used insights gained from performing CRM to reduce the range of input parameters in numerical reservoir simulators.

CRM has been extensively used by authors on many field examples for different purposes. Izgec and Kabir (2009) mentioned the benefits of using CRM compared to solving a transient flow problem. They showed that CRM is applicable even before breakthrough happens and in cases with low injection signal quality. Izgec and Kabir (2010) coupled the CRM and an analytical aquifer model to determine the aquifer influx each well receives. Parekh and Kabir (2011) showed that there is agreement between CRM results and interwell tracer data. They also attempted to use CRM and rate-transient analysis to predict connectivity before breakthrough. Wang et al. (2011) used CRM and satellite images of surface subsidence to explain the performance of a waterflood and suggested reasons for the subsidence. They provided

a surface subsidence model to predict the average surface subsidence based on the injection and production rates. Bansal and Sayarpour (2012) implemented CRM to estimate fault-block transmissibility. Based on the result, they determined the interaction between compartments.

Dinh and Tiab (2008) also implemented multivariate linear regression, but they used fluctuation of bottomhole pressure of both injectors and producers to calculate inter-well connectivity. Lee et al. (2009) estimated finite-impulse-response (FIR) curves corresponding to the fluid flow between all injector-producer pairs to calculate connectivity between them. In this model, production rates are partly determined by the linear combination of surrounding FIR filtered injection rates.

One of the major deficiencies of such methods is their inability to handle changes in flow pattern (Sayarpour, 2008). Change in flow pattern may be a consequence of a long shut-in period for producers or conversion of producers to injectors. Even abrupt changes in injection rates that lead to overpressurizing a region in the reservoir may affect flooding patterns. In these cases the connectivity coefficients are no longer valid. To address this issue, Satter et al. (2007) and Thiele and Batycky (2006) used well allocation factors (WAFs). A well allocation factor is assigned to each injector and is the ratio of the injected fluid volume to the total volume of fluid produced at offset wells (Satter et al., 2007). Thiele and Batycky (2006) state that the well allocation factor is a dynamic value, and it changes with injection and production variations.

Fig. 1 shows streamlines generated by FrontSim® software at different times from a simulation of an example problem used by several authors and described in Albertoni (2002). It is a synthetic field where injection rates in 5 wells fluctuate to study connectivity to the 4 producers in the reservoir. Although the flooding pattern is fixed, the influence of each injector on the producers varies as injection rates fluctuate. In the left figure, a high-pressure region forms around injector 1 (I1) caused by a large amount of injection. This causes the streamlines eminating from injector I3 to avoid this region when flowing towards producers P1 and P2. In the right figure, the region around I2 is now the high pressure region and the streamlines again avoid the high pressure area when flowing towards producers P1 and P3. In each case, injection and production rates in the entire domain and not an individual well, determine the pressure field and the resulting fluid flow direction. Therefore the claim of independency of correlation coefficients from rate may not be appropriate.

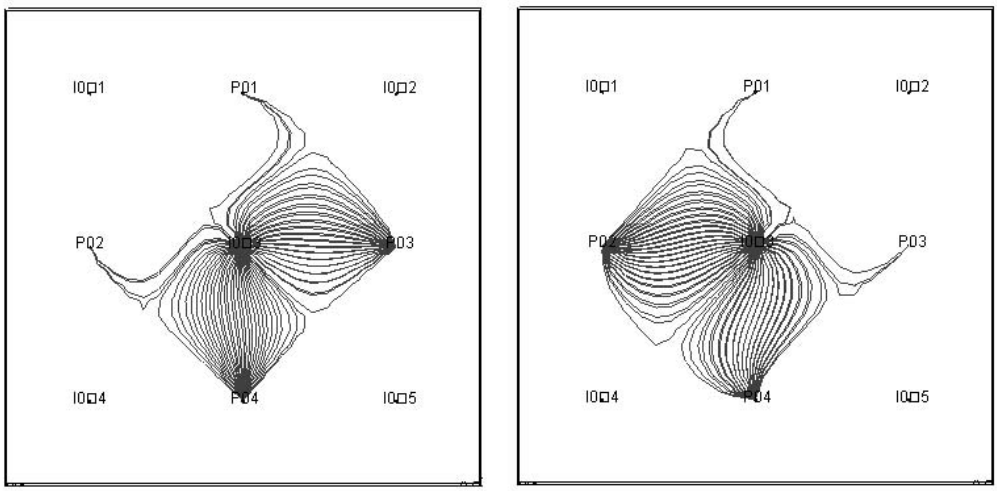

Figure 1: An example of changes to streamlines as the direction of pressure gradients change.

In this research, a tool is developed that uses inverse techniques from automatic history matching, which are simplified such that the numerous grid-block parameters and property characteristics from detailed reservoir characterization are avoided. The amount of input data is reduced to injection and production rates and well positions. Such a parsimonious approach can be applied on reservoirs with minimum data.

The ability to handle changes in flow direction is another characteristic of the model that increases the range of cases that can be studied. Changes in flow direction may be the result of pressurizing certain regions in a reservoir, adding new wells, or shutting-in producers. Permeability and pressure gradient determine flow direction in a reservoir. Since the approach is based on a simulation flow equation, permeability and pressure gradients are included. Therefore it can handle changes in flow direction.

The method is capable of matching one or selected time intervals of production history for an entire field or group of wells. It estimates parameters that can be used to infer permeability variations and geological features in the reservoir. In addition, once parameters are estimated the model can be converted to a predictive tool to estimate total production rates in each producer using injection data as input. Different case studies with different

permeability distributions and/or injection-production scenarios are considered to test the performance of the method under different conditions.

2. Methods

In the approach developed in this work, the reservoir is viewed as a network model consisting of sites and bonds. In standard pore network modeling, sites are equivalent to pore bodies and bonds to pore throats. In this work, the sites correspond to the volumes assigned to each well and bonds to the connection between wells. This assignment is different from how Samier et al. (2001) associated pore volume to each well. They used a streamline simulator and detailed reservoir characterization and found the geometric influence zone around each injector and producer. The influence zone of injectors and producers may overlap but may not cover the whole reservoir.

To construct the model presented in this work, the geometry of the reservoir and well positions are required. The relative distance between the wells and the distance to any of the boundaries determine the volume rather than flow characteristics of the domain. In addition, it covers the whole reservoir. First, characteristics of the model are discussed. Then a flow equation and an optimization method will be developed to find the unknowns in the model.

3. Network Model Construction

This network model as other network models is characterized by three properties:

- Sites (the node volume or the volume assigned to each well)
- The network coordination number (the number of bonds attached to each site)
- Bonds (conductance)

3.1. Sites (Node Volume).

The principal objective here is to represent the domain of a reservoir by a set of tiles each of which contains a well. Each tile has a known surface area and a thickness corresponding to the estimated thickness of the reservoir in the neighborhood of the well. Each tile then represents a node volume and is referred to as V_b in the calculations. Later, it will be explained that if the

reservoir structure is available, it can be used to find the tile thicknesses. The summation of volumes should be equal to the estimated volume of the reservoir. Since the intention is to work with the communicating parts of the reservoir, multiplying the tile areas by net pay results in more realistic node volumes. This volume is constant during the study period and is not a function of rate variations. Therefore it is the true drainage volume of the well only in the case of a homogeneous system with homogeneous rate variations.

In this work, Voronoi tessellation is used to divide the reservoir area into convex polygons. The tiles have a property that any point in the interior of the tile is closer to the well at the center of the tile than to any other well (Farrashkhalvat and Miles, 2003). Voronoi cell generation requires a background grid that is generated by the Delaunay method. The area of the reservoir is the triangulation domain, and well positions are input nodes. Tiles are formed by connecting the circumcenters of the Delaunay triangles. As shown in Fig. 2a, Voronoi cells that are generated only using well positions cannot cover the entire area of the reservoir. The boundaries of the reservoir that are not covered by the triangles must be included in order to calculate realistic node volumes. To include the uncovered areas, the edges of the Voronoi grid are extended to intersect the boundaries. The area surrounded by the boundary of the reservoir and the Voronoi edges are used to calculated node volumes for boundary nodes (Fig. 2b).

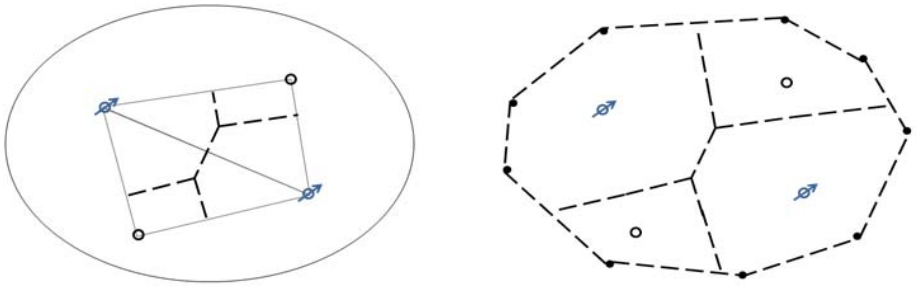

(a) Background grid and Voronoi formed by connecting the center of triangles.

(b) Node volumes formed by extending Voronoi edges.

Figure 2: Node volume assignment.

3.2. Network coordination number.

In porous media, fluid flows along various throats which are connected to each pore. The number of throats connected to each site is called the coordination number Z. With different values of Z, the topology of the porous media can be well defined.

In this work, the coordination number is defined by the number of production wells connected to an injection well. It is the number of production wells that are influenced by an injector well. In this portion of the work injector-injector and producer-producer connections were ignored. The question was, which producing wells are influenced by which injection wells? Obviously, producers likely receive larger volumes from close injectors in homogeneous formations.

Producers that do not have a bond with an injection well are not affected by it. So the more bonds an injection well has, the more likely it will be that distant injector-producer connections that may occur in heterogeneous reservoirs will be seen. Increasing the number of bonds increases the number of unknowns, which consequently increases computational time in the optimization. So there is a tradeoff between the number of bonds and the speed with which a solution is obtained.

To determine the coordination number of an injector, an influence radius can be assigned to it. Then, those producing wells that fall within a circle with that radius of influence centered on the injection well will have bonds with the injector. For problems with a small number of wells, all injectors are connected to producers. For larger problems this radius should be determined. Permeability and porosity of the rock and compressibility of the fluid are the main properties that control the radius of influence (Lee, 1982); since these terms are initially unknown, distance between an injector and a producer is the only parameter that can be used to determine the appropriate radius of influence distance for each connection. Kaviani et al. (2010) adressed a model reduction approach called windowing, which is very similar to what is being done in this work. They used the location of wells to define the window.

3.3. Bonds (Conductance).

Like the role of a throat in pore network modeling, a bond connects node volumes and controls transmissibility between the nodes. In other words, they act as the conduits for fluid flow between injection and production wells. In the pore network modeling literature, this conduit is designated

as the conductance between the centers of pore bodies and is denoted g_{IJ} (Bakke and Øren, 1997). The subscripts denote node volumes I and J. The volumetric flow rate between two connected nodes I and J, q_{IJ} is given by

$$q_{IJ} = g_{IJ}(p_I - p_J) \tag{1}$$

In this approach q_{IJ} represents the flow rate between the connected injector and producer, i and j. For Darcy flow between wells, g_{IJ} will be:

$$g_{IJ} = \frac{k_{IJ}A_{csIJ}}{\mu L_{IJ}} \tag{2}$$

Where k_{IJ}, A_{csIJ}, and L_{IJ} are the average permeability, area open to flow, and conductance path distance between nodes (wells), respectively, and are all properties of the domain. μ is the viscosity and is a fluid property. Since the problem considered here is a two-phase flow system, μ will be the average viscosity of the two phases. Note also that capillary pressure and gravity are ignored in this formulation.

Although distance between wells is a reasonable value for the L in the conductance formula, it may not be representative of the actual path that streamlines travel since it would be the shortest streamline distance between wells. For homogeneous cases this may be a good approximation, but for cases with complex features it likely underestimates the distance.

In this work, it is assumed that A_{cs}, or the cross-sectional area open to flow, is obtained by multiplying the length of the "common edge" of Voronoi cells between adjacent injectors and producers by their average thickness values. This area is not a good representation of the area open to flow. First of all, there is no "common edge" between nonadjacent cells (wells), despite the fact that there may be connection between them. For homogeneous cases, cross-sectional area open to flow depends on the flux between wells, and the flux varies with fluctuations in rate. For nonhomogeneous cases with geologic complexity, the area term may be far different from what is assumed. The impact of these formulation "errors" will be shown to be minimal to the evaluation of interwell connectivity.

In this way, properties between an injector-producer well pair are assigned to the bond that connects corresponding nodes in the network model.

4. Flow Equation

The continuity and Darcy equations are combined, as suggested by Ertekin et al. (2001), to obtain flow equations for the network model. For producer

and injector flow, these equations may be written as:

$$\sum_{I=1}^{Z_j} \beta_c \frac{k_{IJ}}{B\mu} \bigtriangledown p_{IJ} A_{csIJ} + q_{sc} = (\frac{V_b \phi c}{\alpha_c B^0} \frac{\partial p}{\partial t})_J \tag{3}$$

$$\sum_{J=1}^{Z_i} \beta_c \frac{k_{IJ}}{B\mu} \bigtriangledown p_{IJ} A_{csIJ} + q_{sc} = (\frac{V_b \phi c}{\alpha_c B^0} \frac{\partial p}{\partial t})_I \tag{4}$$

I represents the node volume containing injector i, and J represents the node volume containing producer j. Porosity, ϕ, is assumed constant, but B, the formation volume factor (FVF), c, the compressibility, and μ, the viscosity, are pressure dependent. Z_j and Z_i are the producer and injector coordination number, α_c and β_c are volumetric and transmissibility unit conversion factors, and B^0 is the FVF at a reference pressure. V_b is the bulk volume of the node and is obtained by multiplying the node (tile) area by its average thickness. A_{csIJ} is the cross-sectional area open to flow between nodes (wells) I and J and is different from the node or tile area. $\bigtriangledown p_{IJ}$ is the pressure gradient, and k_{IJ} is the average permeability between injector i and producer j that correspond to nodes I and J. For a particular time denoted as $n+1$, the pressure gradient is estimated by

$$\frac{p_J^{n+1} - p_I^{n+1}}{L_{IJ}} \tag{5}$$

The p terms are the node pressures and L is assumed to be the distance between the wells. Substituting the pressure gradients and g_{IJ} into the flow equations gives:

$$\sum_{I=1}^{Z_j} \beta_c (\frac{g_{IJ}}{B^n})(p_J^{n+1} - p_I^{n+1}) + q_{sc} = (\frac{V_b \phi c^n}{\alpha_c B^0})_J \frac{p_J^{n+1} - p_J^n}{\Delta t} \tag{6}$$

for producers and

$$\sum_{I=1}^{Z_i} \beta_c (\frac{g_{IJ}}{B^n})(p_J^{n+1} - p_I^{n+1}) + q_{sc} = (\frac{V_b \phi c^n}{\alpha_c B^0})_I \frac{p_I^{n+1} - p_I^n}{\Delta t} \tag{7}$$

for injectors. The superscript n indicates the time step at which parameters are evaluated. The q_{sc} term is a source when the equation is written for

a producer and a sink when it is written for an injector. In conventional reservoir simulation, q_{sc} is related to the well index, J_w, and the difference between average block pressures and flowing sandface pressures, p_{wf}. In the network model, injection rates are provided and fixed, and production rates are unknowns to be determined by an optimization procedure. The injectivity and bottomhole pressure response of injectors is dampened by the node volumes. Thus the well index for injectors is of minor importance compared to those of producers that control the fluctuating production rates in the producers. Production is a match parameter and is related to the bottomhole pressure in a well by:

$$q_{sc} = -J_w(p_J - p_{wf}) \tag{8}$$

For a case of unknown well index and bottomhole pressure, a large value can be assigned to J_w to reduce the effect of the well, and average reservoir pressure is used for p_{wf}. It is also assumed that for production wells, p_{wf} values are constant. If p_{wf} values are known at various times, these values can be used as additional constraints in the inverse problem solution procedure or to constrain the J_w term to better values.

5. The inverse problem and solution

For the network model, the inverse problem is the problem of determining the conductance between wells from production data measured at producing wells. Injection well rates provide the stimulus, and producing well rates represent observed data. The model is the relationship between the observed data and the model parameters.

To obtain a good solution the difference between observed data and the modeled response must be minimized. In this case, one has to minimize the difference between the observed production and the modeled production response using estimated conductance values. This goal is obtained by minimizing the objective function:

$$D(g) = \frac{1}{2}(q_{mod}(g) - q_{obs})^T C_D^{-1}(q_{mod}(g) - q_{obs}) \tag{9}$$

where q_{mod} is an assumed theoretical model for predicting production for a given g, q_{obs} is a N_D dimensional column vector containing measured production values, C_D is a $N_D \times N_D$ covariance matrix for data measurement

and modeling errors, and g is an N_m-dimensional collumn vector of model variables. N_m and N_D are the number of model variables and the number of observations, respectively.

To minimize Eq. 9 a derivative-free alogorithm is implemented. The derivative free algorithm used in this context is designed for least-square problems of the form:

$$minD = \frac{1}{2}\sum_{n=1}^{N_D}(d^n)^2 \tag{10}$$

where d^n, $n = 1, \cdots, N_D$ are generally nonlinear functions. If the C_D matrix is defined as a diagonal matrix, d^n can be written as:

$$d^n = {q_{mod}}^n - {q_{obs}}^n \qquad n = 1, \cdots, N_D \tag{11}$$

For the nework model, d^n is the difference between observed and model production rates, at time n, and the function value is extracted from simulation. Eq. 11 is written based on the assumption that the components of the data error vector are independent Gaussian random variables with all means equal to zero and variance σ_d.

In this work, a class of the derivative-free method that requires the sequential minimizations of models is implemented. The minimizations are quadratic or linear and are based upon evaluations of the objective function at sample sets (Zhang et al., 2010).

6. Application to synthetic fields

This section examines the application of the technique on a numerically simulated synthetic field. This case was presented by Albertoni and Lake (2003) and has been used by many authors to study well connectivity relationships. The domain is a single-layered reservoir with a closed boundary. A five-spot injection pattern is used to investigate the performance of the method. The case has 5 injectors, 4 at the "corners" of the domain and one in the middle. The 4 producers on the top, bottom, left, and right sides of the domain establish the injection pattern. Oil and water compressibility values are both set to $5 \times 10^{-6} psi^{-1}$, and rock compressibility is ignored. All wells are vertical, and adjacent wells are distanced 800 ft apart. The injection data from Albertoni and Lake (2003) are used as stimulus and production is controlled by the injection rates, since production well BHPs are equal and fixed at 500 psi. The numerical simulator runs for 100 months with $\Delta n = 1$

month. Different permeability distributions and injection senarios are applied to the domain to test the performance of the method under different interwell connection cases.

6.1. Homogenous reservoir.

The first case is a homogenous system with an isotropic permeability of $40\,md$. The numerical values of conductance and fluid flow between injector-productor well pairs are shown in Tables 1a and 1b respectively. Fluid flow between the well pairs is the amount of injection from an injector that influences production in a producer. Once conductance values are calculated, fluid flow is computed by multiplying values of the conductance times the pressure gradient between the wells. Conductance and flow values are shown in Fig. 3. Conductance is represented by the thickness, and flow by darkness of the bonds. The thicker the bond, the larger the value of conductance, and the darker the bond, the larger the volume of fluid that has passed through the bond.

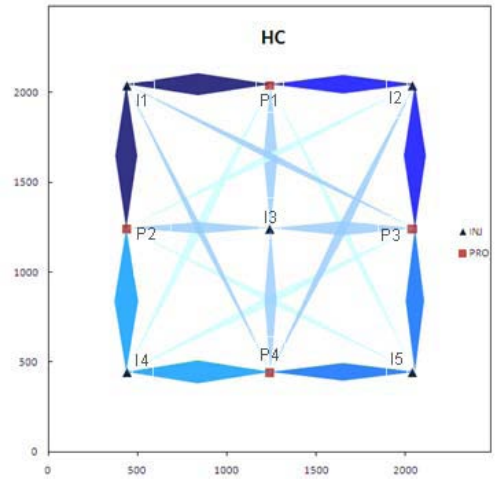

Figure 3: Illustration of the Conductance and flux shown in Table 1a and Table 1b.

Fig. 3 indicates both reservoir and flow properties. Thicker bonds between closer well pairs indicates higher conductance between them. That makes sense, since conductance is inversely related to the distance between wells when permeability is homogeneous. For those wells that are equal distance apart, thicker shapes correspond to higher kA_{cs} values. From Fig. 3 it can be inferred that flow is directly related to g, since the thicker the bond,

Table 1: Homogenous Reservoir.

(a) Conductance ($d.ft/cp$)

	P1	P2	P3	P4
I1	0.271	0.273	0.130	0.124
I2	0.254	0.134	0.266	0.159
I3	0.201	0.182	0.202	0.196
I4	0.159	0.289	0.152	0.272
I5	0.123	0.121	0.240	0.239

(b) Cumulative flow between Wells (bbl)

	P1	P2	P3	P4
I1	58676	59401	28364	27086
I2	42021	22315	44361	26713
I3	23838	21769	24240	23726
I4	14560	26793	14135	25535
I5	17535	17393	34493	34581

(c) kA values ($d.ft^2$)

	P1	P2	P3	P4
I1	216.9	218.6	233.1	221.7
I2	203.1	239.7	212.8	285.0
I3	160.5	145.4	161.5	156.9
I4	283.9	231.1	272.0	217.6
I5	220.4	217.0	192.2	191.5

(d) Average well allocation factors

	P1	P2	P3	P4
I1	0.338	0.342	0.163	0.156
I2	0.310	0.165	0.328	0.197
I3	0.255	0.233	0.259	0.254
I4	0.180	0.331	0.174	0.315
I5	0.169	0.167	0.332	0.333

the darker it becomes. That makes sense also, since flow is directly proportional to g. This explains why the closer the wells are, the larger the amount of fluid flow between them. The darkness of bonds connected to an injector also depends on the amount of water injected, which in this case show that the darkness is consistent with injection rates.

Table 1c shows kA_{cs} values, which are obtained by multiplying the conductance by the viscosity and the distance between wells. Average well allocation factors are presented in Table 1d. The average well allocation factors are the fractions of water injected that influence production in a producing well (Thiele and Batycky, 2006). In other words, it is obtained by dividing values of each row of Table 1b by the sum of values in that row.

One of the important characteristics of Albertoni and Lake (2003) and Yousef et al. (2006), as they pointed out in their papers, is the estimation of symmetric values for connectivity. They concluded that symmetry indicates

that weights do not depend on injection rate. In their work, connectivity weight, which is the fraction of injection rate that goes to a producer, shows a symmetric behavior, but the time constant, which includes productivity and pore volume of the producer, is not as symmetric. In this work, the well allocation factors obtained are symmetric, but conductivity values are not as symmetric as well allocation factors. Thus it can be concluded that conductance values depend on injection rates. Since k is constant and homogeneous and the wells are equally spaced (L values are constant), the only property that the calculated rate depends on should be A_{cs}. A_{cs} is defined to be the area open to flow, or in other words, a cross section of the reservoir between the injector and producer well pair. One can compare A_{cs} values with the number of streamlines between well pairs. In a homogeneous case the number of streamlines between a well pair and the area covered by them is proportional to the flow between the wells. When injection rates fluctuate, the flow between the wells and the number and area covered by streamlines change as well. Therefore, one may conclude that A_{cs} values are proportional to the flow and change as the rate fluctuates. As a result, one expects that conductance values between I1 and producers to be larger than conductance values between I4 and producers since injection rates are lower in I4. However, the values of Table 1c do not confirm this hypothesis. Values of kA_{cs} for I4 are relatively higher than other injectors, in spite of higher injection rates in I1. The smaller pressure gradient between I4 and the producers is the reason for the slightly higher conductance values around I4. Table 1d also shows good symmetry. Injector I2 shows an asymmetric behavior, since injection in I1 is comparatively higher than in I4. Therefore flow goes toward the producers with less support.

6.2. Presence of barriers.

The method can recognize the introduction of a sealing fault into the model. A sealing fault in the Albertoni and Lake (2003) homogeneous system was modeled. The sealing fault was created by setting the transmissibility multiplier to 0 between certain grid cells. Albertoni and Lake (2003) obtained negative connectivity values for injector-producer pairs on different sides of a similarly simulated fault. The results of the network model for this system are shown in Fig. 4. Conductance values corresponding to pairs of wells located on each side of the fault are zero. The volume of fluid flowing between them is very small compared to flow between other well pairs. This shows no

conduction between injection wells and production wells that are separated by the fault.

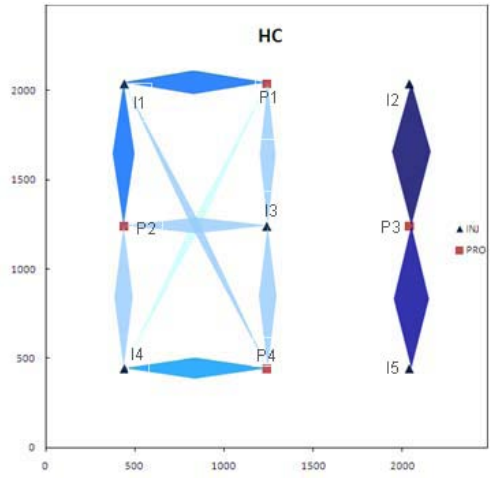

Figure 4: Illustration of the Conductance and flux for a case with a barrier.

6.3. Anisotropy.

In this case, permeability in the y direction for each grid cell was set to $\frac{1}{10}$ the permeability in the x direction. Fig. 5 shows that both conductance and flux are larger in the x direction, indicating that permeability is higher in that specific direction. Unlike the homogenous case, the effect of injection rate on kA_{cs} values is more tangible. The largest volume of fluid has passed between pairs I1-P1 and I2-P1.

6.4. Complex Geologic features.

Complex geologic features are very common in reservoir studies. Because of these features, streamlines may travel different paths that are not the straight line that connects injection to production wells. Therefore conductance values should be interpreted with more consideration. In this example, a channel structure with permeabiliy that is 10 times larger than the rest of the reservoir model connects injection well 2 to production well 2 (Fig. 6a). Since production well 2 is placed in a highly permeable region, it has higher productive capabilities. Fig. 6b is plotted using the FrontSim® software with model parameters other than the permeability values identical to the homogeneous case. As shown in Fig. 6b, more streamlines end at production well

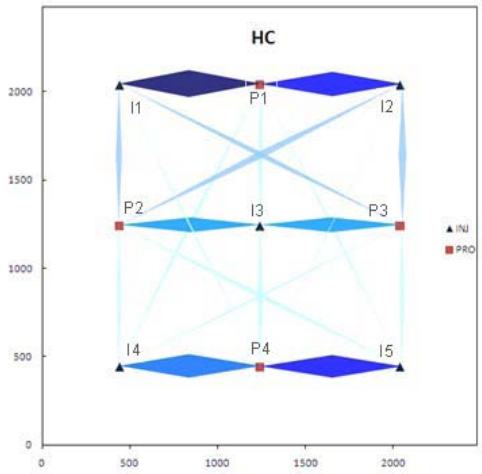

Figure 5: Illustration of the Conductance and flux for a case with an anisotropy.

2, and nonadjacent wells have considerable contribution. Fig. 7 shows the network model result for this case. Although one cannot infer the shape of the channel from the conductance values, the existance of some anomaly around production well 2 is noticable. In comparison to Fig. 3, all the injection wells have much stronger influence on production well 2 than in the homogeneous case. All of the other producers are receiving significently less support, which indicates the heterogeneity is more widespread that just in the region around producer 2 and is a "regional trend".

6.5. Closed Well.

Shutting in a producer or adding a new well to the system is fairly routine in waterflooding. Coefficients calculated by currently available methods are only valid when a fixed number of producers and injectors is being studied. Once a well is added or removed from the system, coefficents are no longer valid and need to be redetermined. This limits the current methods to cases where there are sufficient continuous data from the active wells. In the situation where all wells are producing, all nodes have a sink representing the producing well. Once a production well is shut in, the sink is removed but the node is still interacting with other nodes through the bonds. This helps to study broader time intervals and includes those times when wells are shut in.

This methodology can be shown using the homogeneous case of example 1. Production well 1 was added to the system after 30 months of field production

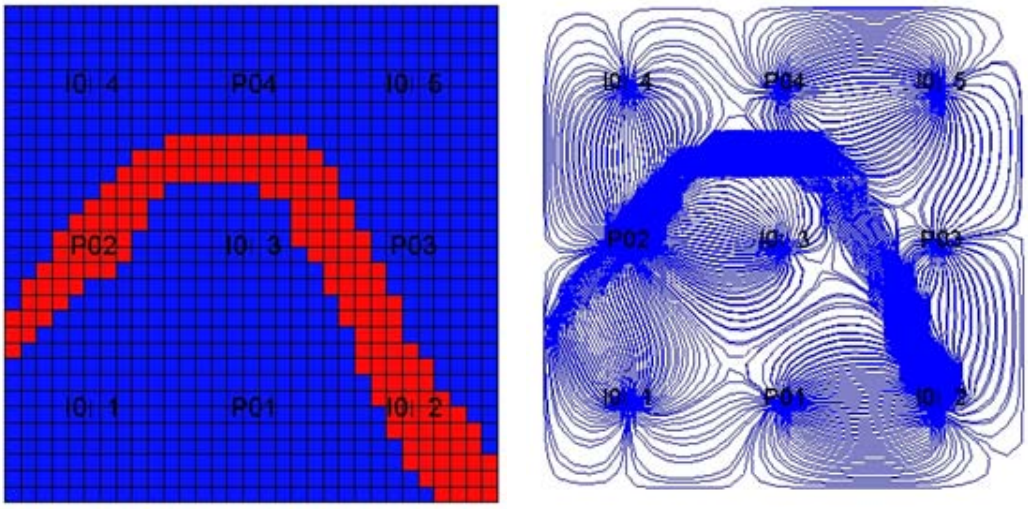

(a) Permeability distribution in the domain..

(b) Distribution of streamlines in the domain.

Figure 6: A case with geological complexity.

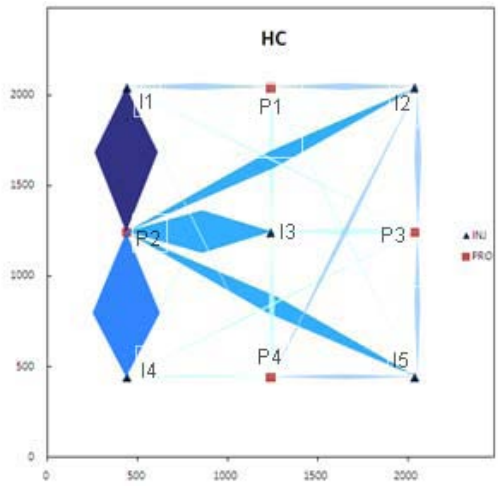

Figure 7: High permeable channel: Conductance values.

and was produced for the next 20 months. Then production data during the first 50 months were used to predict production for the next 50 months. Taking advantage of the whole production period, the network model predicts

Table 2: Yield R^2 for production prediction when one well is added to the system

	P1	P2	P3	P4
Albertoni and Lake (2003)	0.893	0.924	0.965	0.957
Yousef et al. (2006)	0.996	0.990	0.956	0.979
Network model	0.999	0.998	0.993	0.998

production better than other methods.

In the network model the production data during 50 timesteps including the first 30 timesteps when 3 producers were active are studied to predict the next 50 timesteps when 4 producers are active. The CM and RM method are unable to use the first 30 timesteps and are limited to the 20 timesteps when all 4 producers were active. Therefore, the network model provides the opportunity to study a broader time inerval, which results in a more robust prediction. Table 2 shows the correlation coefficient (R^2) values for production prediction for the 50 time-step interval.

6.6. 16×25 Synfield.

To test the performance of the network model on a larger scale, a homogenous field with a larger number of wells was studied. This case has 16 production and 25 injection wells. Wells are positioned on a 5-spot pattern, and the distance between injector-producer well pairs is 890 ft. Injectors are shown by triangles, and producers are represented by circles and are numbered from the top left. A history of 65 months, which consists of 1040 data points was generated using the injection history and parameter values of the example presented for the homogeneous reservoir model. Conductance values shown in Fig. 8a for injectors I7, I8, I14, I17, and I19 are much higher than the rest of the values. Injectors at the corners also demonstrate higher conductance values reflecting the no flow boundary conditions.

To insure that values are not just local minima of the objective function, a case with symmetric injection rates was tested. Injection rates in all wells were all equal. For this case, the calculated conductance values are symmetric and indicate the homogeneity of the system (Fig. 8b). This indicates that obtaining asymmetric conductivity values is the response of the system to the production and injection rate variations. Note that the computed WAFs show a homogenous media in spite of the asymmetric conductance values

shown in Fig. 8a.

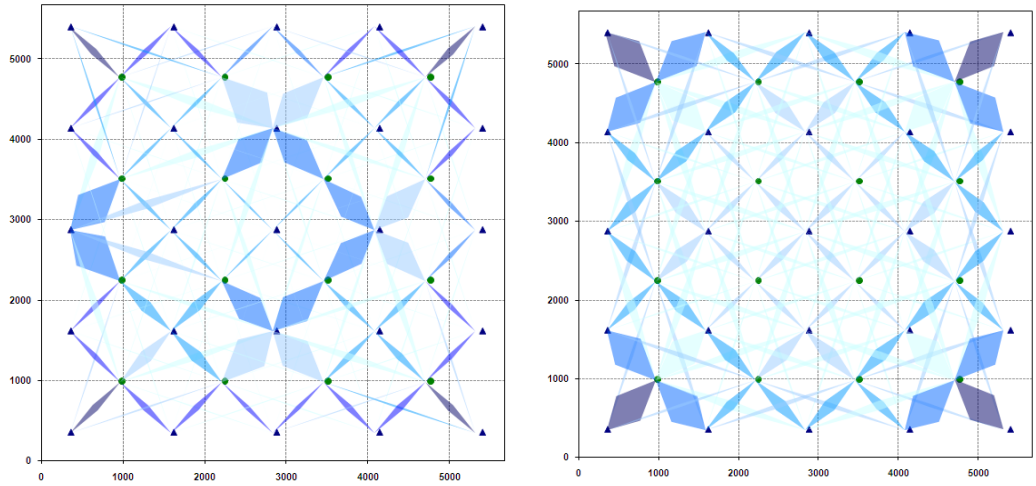

(a) Fluctuating rates. (b) Constant rate.

Figure 8: Conductance and flux for a homogeneous case with 16× 25 wells.

7. Influence of data quality and assumptions

When estimating reservoir parameters, the output from the method can be improved significantly by using better quality data and adding more data to the system. For example, the addition of or improving the accuracy of boundary distances, fault positions and/or more accurate well indices for producing wells results in estimation of more realistic node volumes and helps to infer communication between the node and the well which improves the estimated conductivity values relative to values used to generate the response. For the homogeneous case, using well index values from the simulation software used to generate the rate profile reduces the difference between observed and model production by 30% over the result obtained using very large well index values. The new conductance values (Tables 3a) are twice those found with the large well indices presented in Tables 1a. Well allocation factors (Tables 3b) show that injectors have a slightly higher influence on adjacent wells compared to the same case when large well index values were used. Note that for the caes we have studied, relative values for both conductance and well allocation factor lead to similar interpretations for the degree of

connectivity between wells whether the "incorrect" or the "correct" parameter values are used. When the system is used to try to estimate physical properties rather than well-to-well influence, the more accurate input data is required.

Table 3: Model with known WI.

(a) Conductance ($d.ft/cp$)

	P1	P2	P3	P4
I1	0.771	0.773	0.244	0.242
I2	0.815	0.259	0.814	0.260
I3	0.577	0.582	0.584	0.589
I4	0.284	0.877	0.284	0.875
I5	0.227	0.231	0.724	0.732

(b) Well allocation factors

	P1	P2	P3	P4
I1	0.371	0.381	0.123	0.125
I2	0.364	0.122	0.386	0.129
I3	0.229	0.245	0.255	0.271
I4	0.113	0.363	0.124	0.400
I5	0.109	0.117	0.377	0.397

7.1. Well index and bottomhole pressure.

Bottomhole pressure (BHP) and well index (WI) are two important sources of uncertainty in the network model. If the producer WI is assumed to be a value that is too low or if the producer BHP value is assumed to be too high (relative to actual values), the predicted flow to a producer will be lower than actual. Similarly, assumed values for WI that are too high or assumed values for producer BHP that are too low increase the amount of flow to a producer. Both parameters influence the connectivity value calculation and therefore near-well permeability interpretation.

The effect of using incorrect BHP on conductance and well allocation factor is studied by comparing two cases. In both cases, the same simulated injection scenario was applied and the permeability field was homogeneous, but a different BHP value was assigned to one of the producers. All producers were assumed to be producing under a 500 psi BHP constraint, except producer 2, which was producing with a 600 *psi* BHP constraint. The difference is that in case one, the BHP difference is known and accounted for, but in case two it is assumed that all producers are producing at the 500 *psi* BHP.

Table 4: Different BHP at producer 2.

(a) Conductance ($d.ft/cp$)

	P1	P2	P3	P4
I1	0.792	0.789	0.242	0.239
I2	0.857	0.253	0.840	0.267
I3	0.658	0.650	0.659	0.671
I4	0.325	0.973	0.315	1.002
I5	0.219	0.218	0.718	0.731

(b) Average well allocation factors

	P1	P2	P3	P4
I1	0.386	0.366	0.124	0.124
I2	0.372	0.106	0.394	0.129
I3	0.239	0.208	0.268	0.285
I4	0.120	0.311	0.131	0.437
I5	0.108	0.099	0.386	0.406

For case one, well allocation factors are smaller for producer 2 (Table 4a and 4b). Conductance values do not show heterogeneity, which is a good indication of a homogenous field and different bottomhole pressure. For a homogeneous case, if an incorrect BHP is used (case two), depending on whether a higher or a lower pressure is used, larger or smaller conductance values are obtained for that specific well (Table 5a and 5b). Smaller or larger conductance values are the response of the model to compensate for the higher or lower pressure difference between injector-producer pairs. For example in case two, the BHP that is assigned to producer 2 is less than the actual BHP of the well. The obtained conductance values for producer 2 are smaller compared to conductance values in case one to reduce the effect of the incorrect higher pressure difference between the well and the node.

The same statment applies to WI. For example, if an incorrect higher WI is used for producer 2, smaller values of conductance are obtained to compensate for the incorrect higher communication between the well and the node.

This comparison shows that using incorrect values of BHP and WI still provide correct values of WAFs. However, any errors in estimation of the actual physical parameters for a producer results in similar errors in the obtained conductance values for that well.

7.2. Node volume and compressibility.

Like BHP and WI, node volumes and fluid compressibility influence the calculated parameters. In this section, node volumes are underestimated by 30%, and the influence of the underestimation on conductance values and

Table 5: Incorrect BHP at producer 2.

(a) Conductance ($d.ft/cp$)

	P1	P2	P3	P4
I1	0.779	0.708	0.255	0.257
I2	0.785	0.152	0.769	0.269
I3	0.568	0.448	0.563	0.580
I4	0.342	0.594	0.320	0.889
I5	0.229	0.209	0.713	0.727

(b) Average well allocation factors

	P1	P2	P3	P4
I1	0.372	0.370	0.128	0.131
I2	0.379	0.083	0.395	0.143
I3	0.237	0.226	0.259	0.278
I4	0.140	0.296	0.144	0.420
I5	0.111	0.119	0.375	0.395

WAFs is studied. The results are shown in Table 6 and should be compared with conductance values and WAFs presented in Table 3. Underestimating reservoir volume results in lower computed conductance values. The situation speeds up the movement of the pulse generated by injection fluctuations to the producers, and computed conductance values are lowered to delay this process. WAFs also show less adjacent injector-producer support. Error in reservoir fluid compressibility estimation influences the conductance values and WAFs in the same way.

The results show that conductance values and WAFs are sensitive to node volume and compressibility, and misestimating these inputs influence the set of obtained parameters. However, misestimating the parameters does not change the inferred well-to-well influence and decision making based on these inferences should be identical to decisions made with ideal parameter estimates.

7.3. Pressure and saturation dependent properties.

Average reservoir pressure in a waterflood is a function of the total injection and production. It increases or decreases in nonlinear ways. Differences in properties of the reservoir fluids cause this nonlinearity. Viscosity and compressibility differences and the shapes of relative permeability curves are factors that influence the average reservoir pressure. These factors may increase or reduce the resistance to flow between injectors and producers. High resistance to flow increases and low resistance to flow decreases the average reservoir pressure for a given injection scheme.

Table 6: Incorrect node volume.

(a) Conductance ($d.ft/cp$)

	P1	P2	P3	P4
I1	0.360	0.361	0.148	0.148
I2	0.382	0.158	0.382	0.158
I3	0.271	0.274	0.275	0.278
I4	0.174	0.408	0.174	0.407
I5	0.139	0.143	0.341	0.345

(b) Average well allocation factors

	P1	P2	P3	P4
I1	0.350	0.354	0.147	0.149
I2	0.346	0.147	0.356	0.151
I3	0.238	0.247	0.253	0.262
I4	0.143	0.345	0.150	0.362
I5	0.139	0.145	0.352	0.364

As noted previously, in order to simplify the problem, it was assumed that fluids with identical properties are injected and produced in the previous examples. The compressibility and viscosity of both fluids were equal ($5 \times 10^{-6} psi^{-1}$ and 1 cp), and linear relative permeability curves were implemented to model the displacement. In a linear relative permeability curve, relative permeability is a linear function of saturation ($k_{rw} = S_w, k_{rnw} = S_{nw}$).

Once these conditions hold, one can assume that resistance to flow is constant, and average reservoir pressure is only a function of total fluid throughput and withdrawal. In practice, saturation-dependent properties like relative permeability are changing as the saturation distribution changes and are most often non-linear functions. Relative permeabilty alteration influences effective permeabilty, injectivity, and productivity of wells. This changes resistance to flow, and as a result average reservoir pressure. When resistance to flow is constantly changing, one set of conductance values should not be expected to model the whole study period. Changing average reservoir pressure also will change the compressibility and viscosity, which are assumed to be constant in the network model.

The effects of a realistic relative permeability curve on conductance value determination is studied by using the relative permeability relationship from model 2 of the SPE comparative solution project (SPECSP) by Christie and Blunt (2001). Other properties were held constant. In SPECSP, the sum of the relative permeability of water and oil is less than 1 (the sum of the effective permeability of the fluids is less than when using linear relative

permeability curves). This causes more resistance to flow as compared to the linear relative permeability case. Identical injection histories were used, so the higher resistance to flow in the non-linear system increases the average reservoir pressure.

Reduction in effective permeability should decrease the conductance values. To test this hypothesis, a case with linear relative permeability curve is compared with a case that uses the SPECSP relative permeability values. Comparing values in Tables 7 with those in Tables 3 shows that there was a 100% reduction in computed conductance due to the reduction of the effective permeability to account for relative permeability effects. This decline varies, depending on the shape of the relative permeability curves and saturation changes

Table 7: Conductance for single phase homogenous reservoir with SPECSP relative permeability ($d.ft/cp$)

	P1	P2	P3	P4
I1	0.323	0.304	0.132	0.080
I2	0.293	0.144	0.324	0.184
I3	0.241	0.226	0.237	0.250
I4	0.178	0.328	0.171	0.358
I5	0.100	0.107	0.248	0.286

through time. What is calculated in the network model as conductance is then an average effective permeability during the study period.

Like relative permeability, viscosity is a part of the conductance term, and its variation changes the computed conductance value, especially when the viscosity difference between the displacing and the displaced phase is significant. Relative permeability is directly a function of phase saturation and the average viscosity of the flow is dependent on the amount of each phase in the flow stream. This means that computed conductance values are also functions of phase saturation and change as the saturations change. In the network model, one set of conductance values is obtained for the entire study period. Therefore, one needs to find a period in which pressures and saturations vary linearly with injection. That is why mature waterfloods are

considered better candidates for the application of these low data requirement tools.

8. Summary and Conclusions

In this research reservoirs are modeled as a number of nodes containing a well. Flow between nodes is through bonds or throats, which are controlled by conductance between nodes. Conductance is directly proportional to effective permeability and cross-sectional area open to flow between wells and inversely related to the distance between the wells. To obtain conductance values, three classes of data are required. The first and main group is production and injection data and well position, which are usually available with some degree of certainty. The second group are those data for which rough estimates of the actual values suffice. They include the location of the boundary of the reservoir, average porosity, bottomhole pressures, and productivity indicies of the wells. The third group are those that are not necessary, but considering them improves the quality of the result.

The results show that incorrect values of BHP and WI give correct values of WAFs, but the error will be reflected in computed values of conductance. Errors in estimating reservoir volume and compressibility will be more widespread and influence the entire set of conductance values and WAFs. In spite of errors and uncertainties in the input parameters of the network model, which is a part of every reservoir study project and previous connectivity models, results are useful and can be relied on. What differentiates a reliable network model is whether it leads to better decisions. All of the solutions thus far were obtained by using different sets of uncertain parameters and in spite of minor differences in the degree of influence between well pairs, show the same connections and lead to consistent decisions.

The method is fast and can be easily set up. It resolves some of the limitations that currently available methods have. It calculates conductance values, which have a physical meaning that still must be interpreted. This approach considers changes in flow pattern due to shuting-in a producer for a long time, adding or removing wells, or changing well rates. This allows the method to study a broader time span. It also allows testing a wider range of injection-production scenarios in the prediction phase.

9. Acknowledgements

This paper is the revised and extended version of SPE 153386 presented at the SPE Western North American Regional Meeting held in Bakersfield, California, USA, 19-23 March 2012. We thank Mr. Shah Kabir and Dr. Matt Honarpour of Hess Corporation for their interest and invaluable comments on this research.

10. Nomenclature

Roman Symbols

A_{csIJ}	area open to flow between two connected nodes I and J (ft^2)
B	formation volume factor (RB/STB)
c	comressibility $(1/psi)$
C_D	$N_m \times N_m$ covariance matrix for the data measurement
g_{IJ}	conductance between two connected nodes I and J $(d.ft/cp)$
J_w	productivity index $(STB/day/psi)$
k_{IJ}	permeability between two connected nodes I and J (d)
L_{IJ}	distance between two connected nodes I and J (ft)
N_D	number of observations
N_m	number of variables
p	pressure (psi)
q_{IJ}	volumetric flow rate between two connected nodes I and J (bbl)
q_{mod}	assumed theoretical model for predicting data measurement (STB)
q_{obs}	N_D dimensional column vector containing measured data (STB)
V_b	bulk volume of the node (ft^3)
Z	coordination number

Greek Symbols

α_c	volumetric conversion factor (5.615)
β_c	transmissibility conversion factor (1.127)
μ_{IJ}	viscosity between two connected nodes I and J (cp)
ϕ	porosity

Indices and Special Subscripts

I	=	node volume containing injector i
J	=	node volume containing producer j
i	=	injector index
j	=	producer index
o	=	oil
w	=	water

11. References

Albertoni, A., 2002. Inferring interwell connectivity from well-rate fluctuations in waterfloods. Master's thesis, The U. of Texas at Austin.

Albertoni, A., Lake, L. W., February 2003. Inferring interwell connectivity only from well-rate fluctuations in waterfloods. SPE Reservoir Evaluation and Engineering 6 (1), 6–16.

Bakke, S., Øren, P. E., January 23 1997. 3-d pore-scale modelling of sandstones and flow simulations in the pore network. SPE Journal 2 (14), 136–149, sPE-35479-PA.

Bansal, Y., Sayarpour, M., 8-10 October 2012. Fault-block transmissibility estimation using injection and production data in waterfloods. In: SPE Annual Technical Conference and Exhibition. San Antonio, Texas, sPE-159067-MS.

Christie, M., Blunt, M., August 2001. Tenth spe comparative solution project: A comparison of upscaling techniques. SPE Reservoir Evaluation and Engineering 4 (4), 308–317.

Dinh, A. V., Tiab, D., September 21-24 2008. Interpretation of interwell connectivity tests in a waterflood system. In: SPE Annual Technical Conference and Exhibition. Denver, Colorado, sPE-116144-MS.

Ertekin, T., Abou-Kassem, J., King, G., 2001. Basic Applied Reservoir Simulation. Society of Petroleum Engineers, Richardson, Texas.

Farrashkhalvat, M., Miles, J., 2003. Basic Structured Grid Generation with an introduction to unstructured grid generation. Butterworth Heinemann, Oxford.

Izgec, O., Kabir, C., 24-26 March 2009. Establishing injector-producer connectivity before breakthrough during fluid injection. In: SPE Western Regional Meeting. Jose, California, sPE-121203-MS.

Izgec, O., Kabir, S., April 2010. Quantifying nonuniform aquifer strength at individual wells. SPE Reservoir Evaluation and Engineering 13 (2), 296–305.

Kaviani, D., Jensen, J. L., Lake, L. W., Fahes, M., November 3-6 2008. Estimation of interwell connectivity in the case of fluctuating bottomhole pressures. In: Abu Dhabi International Petroleum Exhibition and Conference. Abu Dhabi, UAE, sPE-117856-MS.

Kaviani, D., Valko, P., Jensen, J., April 24-28 2010. Application of the multiwell productivity index-based method to evaluate interwell connectivity. In: SPE Improved Oil Recovery Symposium. Tulsa, Oklahoma, sPE-129965-MS.

Lee, J., 1982. Well Testing. Society of Petroleum Engineers.

Lee, K.-H., Ortega, A., Nejad, A. M., Jafroodi, N., Ershaghi, I., March 24-26 2009. A novel method for mapping fractures and high permeability channels in waterfloods using injection and production rates. In: SPE Western Regional Meeting. San Jose, California, sPE-121353-MS.

Panda, M., Chopra, A., February 17-19 1998. An integrated approach to estimate well interactions. In: SPE India Oil and Gas Conference and Exhibition. New Delhi, India, sPE-39563-MS.

Parekh, B., Kabir, C. S., 30 October-2 November 2011. Improved understanding of reservoir connectivity in an evolving waterflood with surveillance data. In: SPE Annual Technical Conference and Exhibition. Denver, Colorado, sPE-146637-MS.

Refunjol, B., Lake, L. W., March 2-4 1997. Reservoir characterization based on tracer response and rank analysis of production and injection rates. In: Forth International Reservoir Characteristics Technical Conference. Houston, Texas.

Samier, P., Quettier, L., Thiele, M., February 11-14 2001. Applications of streamline simulations to reservoir studies. In: SPE Reservoir Simulation Symposium. Houston, Texas, sPE-66362-MS.

Satter, A., Iqbal, G. M., Buchwalter, J. L., 2007. Practical Enhanced Reservoir Engineering. PennWell Corp, Tulsa, Oklahoma.

Sayarpour, M., 2008. Development and application of capacitance-resistive models to water/co2 flood. Ph.D. thesis, The U. of Texas at Austin.

Thiele, M. R., Batycky, R. P., April 2006. Using streamline-derived injection efficiencies for improved waterflood management. SPE Reservoir Evaluation and Engineering 9 (2), 187–196, sPE-84080-PA.

Wang, W., Patzek, T. W., Lake, L. W., 30 October-2 November 2011. A capacitance-resistive model and insar imagery of surface subsidence explain performance of a waterflood project at lost hills. In: SPE Annual Technical Conference and Exhibition. Denver, Colorado, sPE-146366-MS.

Yousef, A. A., Gentil, P., Jensen, J. L., Lake, L. W., December 2006. A capacitance model to infer interwell connectivity from production- and injection-rate fluctuations. SPE Reservoir Evaluation and Engineering 9 (9), 630–646, sPE-95322-PA.

Zhang, H., Conn, A. R., Scheinberg, K., December 2010. A derivative-free algorithm for least-aquares minimization. SIAM J. OPTIM. 20 (6), 3555–3576.